Dissecting Mg II and Fe II emission lines in intermediate redshift quasars with SALT

Raj Prince

Center for Theoretical Physics
Warsaw, Poland

Collaborators: **Bożena Czerny**, Swayamtrupta Panda, Michal Zajaček, Mary Loli Martinez-Aldama, Krzysztof Hryniewicz+++

14th SCSLSA, Serbia, 20 June 2023

NARODOWE CENTRUM NAUKI

erc European Research Council

cft pan

Outline

- AGN and its surrounding
- Modeling Mg II and Fe II emission lines
- Reverberation Mapping: Radius-Luminosity relation for broad-line region

AGN and its surrounding

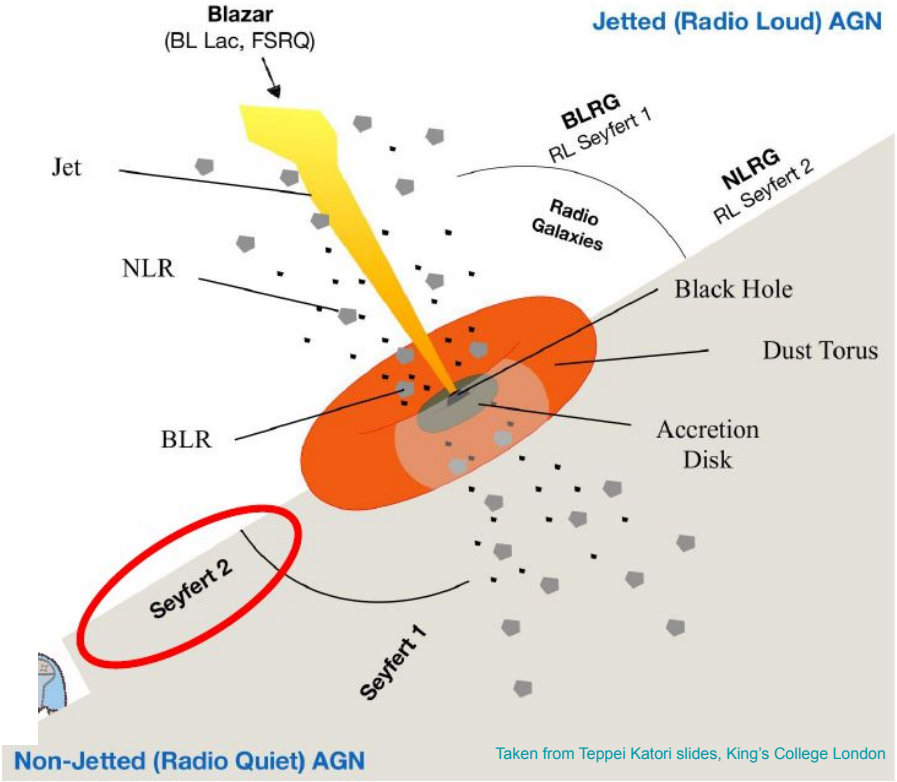

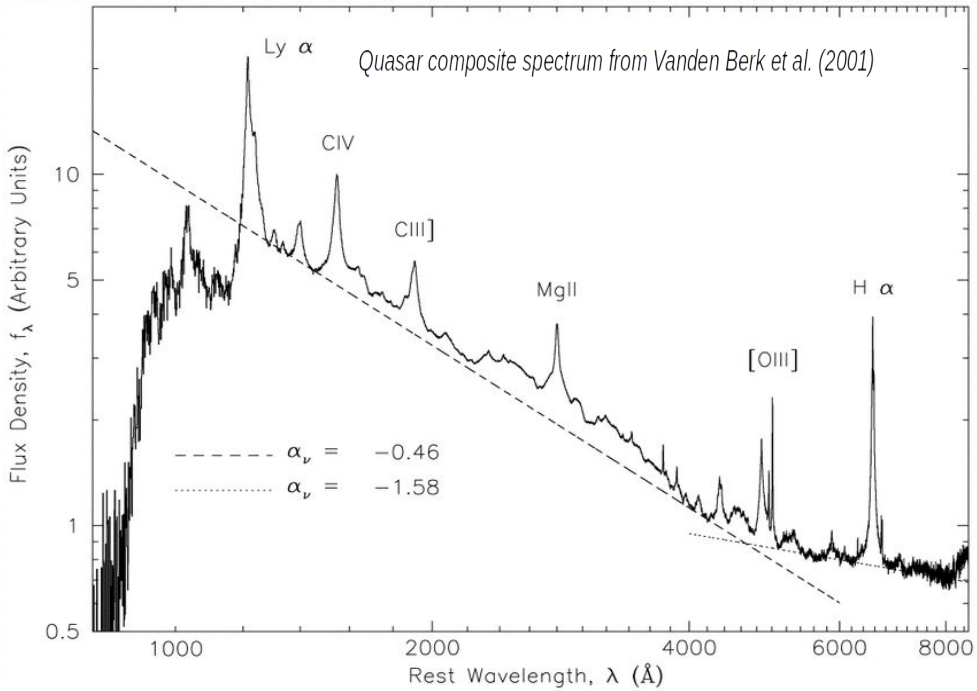

Our SALT monitoring

- Our monitoring started in 2012. We selected three intermediate redshift (z ~ 1) bright quasars
- Our main objective was to measure the emission line time delays and hence only 5 observations per year were proposed
- Observations were done with RSS (Robert Stobie Spectrograph), in slit mode, always 2 exposures of about 800s each
- We collected so far: 42 spectra for CTS, 32 for HE 0413, and 30 for HE 0435

Table 1: Objects selected for further monitoring.

Source	RA	Dec	V	z	observ. month semester I	observ. month semesterII
HE 0413-4031	4 15 14.496	-40 23 40.92	16.5	1.389	July, Sept	Nov,Jan,Feb/March
CTS C30.10	4 47 19.896	-45 37 36.84	16.9	0.910	July, Sept	Nov,Jan/Feb/March
HE 0435-4312	4 37 11.808	-43 06 2.88	17.2	1.232	July, Sept	Nov,Jan,Feb/March

Spectral Modeling

- Our monitoring is focused on Mg II emission line. This is a strong emission line similar to Hβ but located at 2800 Å at rest frame.
- Spectral modeling is done for a narrow band 2700-2900 Å in the rest frame
- Spectrum consists of three basic components: a power-law continuum, broad Mg II emission line, and Fe II pseudo-continuum
- Mg II is described by Gaussian or Lorentzian profile
- For Fe II many templates were tried from Bruhweiler & Verner (2008)

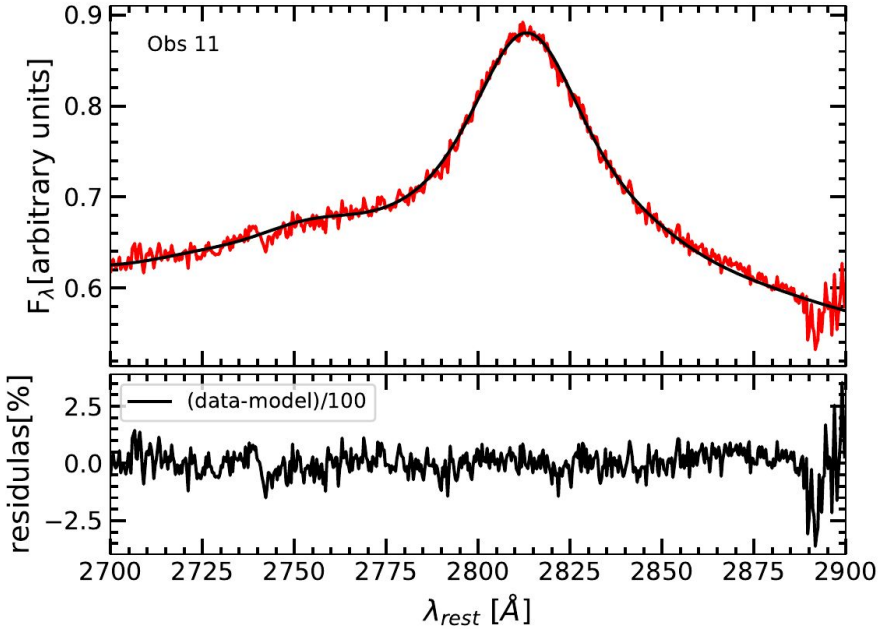

Spectral Modeling

- Our monitoring is focused on Mg II emission line. This is a strong emission line similar to Hβ but located at 2800 Å at rest frame.
- Spectral modeling is done for a narrow band 2700-2900 Å in the rest frame
- Spectrum consists of three basic components: a power-law continuum, broad Mg II emission line, and Fe II pseudo-continuum
- Mg II is described by Gaussian or Lorentzian profile
- For Fe II many templates were tried from Bruhweiler & Verner (2008)

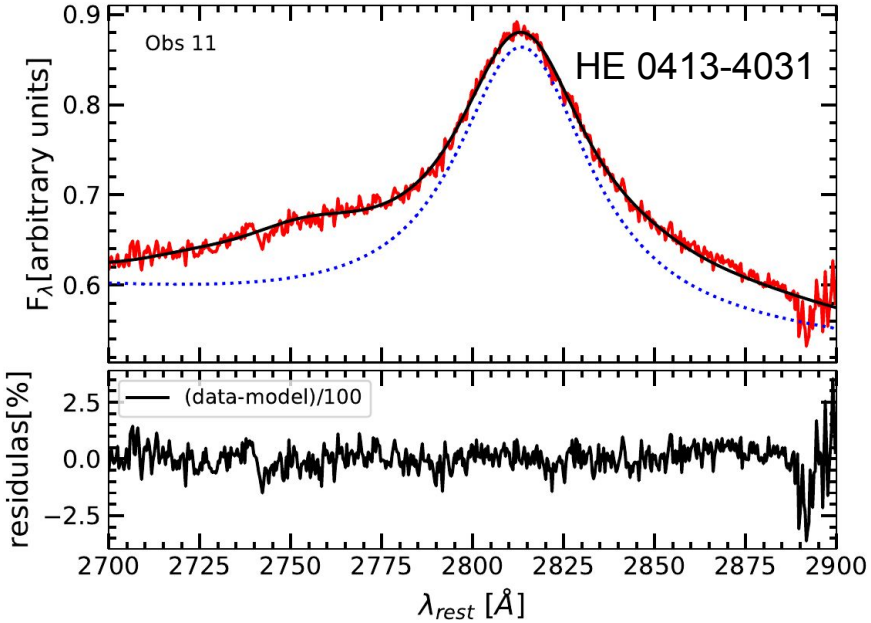

Spectral Modeling

- Our monitoring is focused on Mg II emission line. This is a strong emission line similar to Hβ but located at 2800 Å at rest frame.
- Spectral modeling is done for a narrow band 2700-2900 Å in the rest frame
- Spectrum consists of three basic components: a power-law continuum, broad Mg II emission line, and Fe II pseudo-continuum
- Mg II is described by Gaussian or Lorentzian profile
- For Fe II many templates were tried from Bruhweiler & Verner (2008)

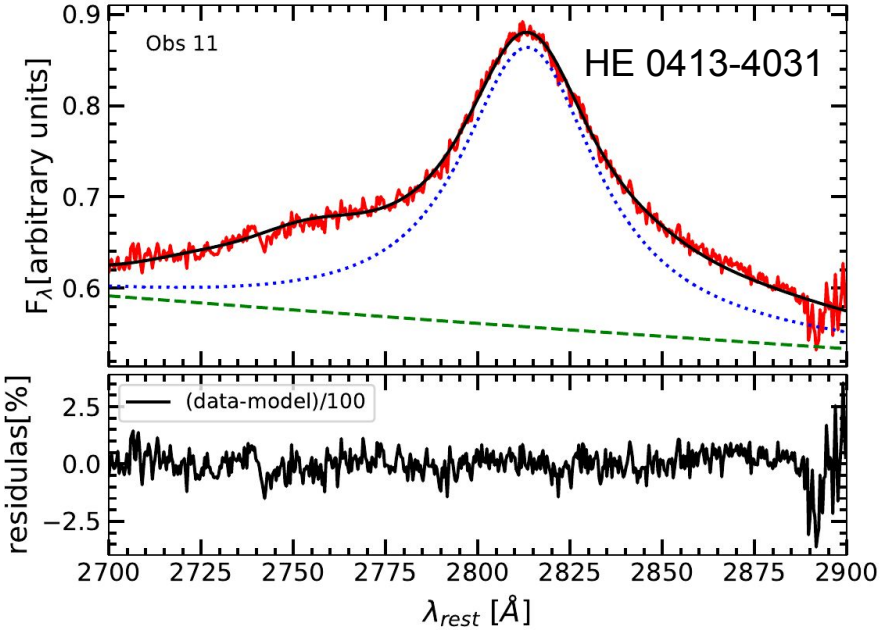

Spectral Modeling

- Our monitoring is focused on Mg II emission line. This is a strong emission line similar to Hβ but located at 2800 Å at rest frame.
- Spectral modeling is done for a narrow band 2700-2900 Å in the rest frame
- Spectrum consists of three basic components: a power-law continuum, broad Mg II emission line, and Fe II pseudo-continuum
- Mg II is described by Gaussian or Lorentzian profile
- For Fe II many templates were tried from Bruhweiler & Verner (2008)

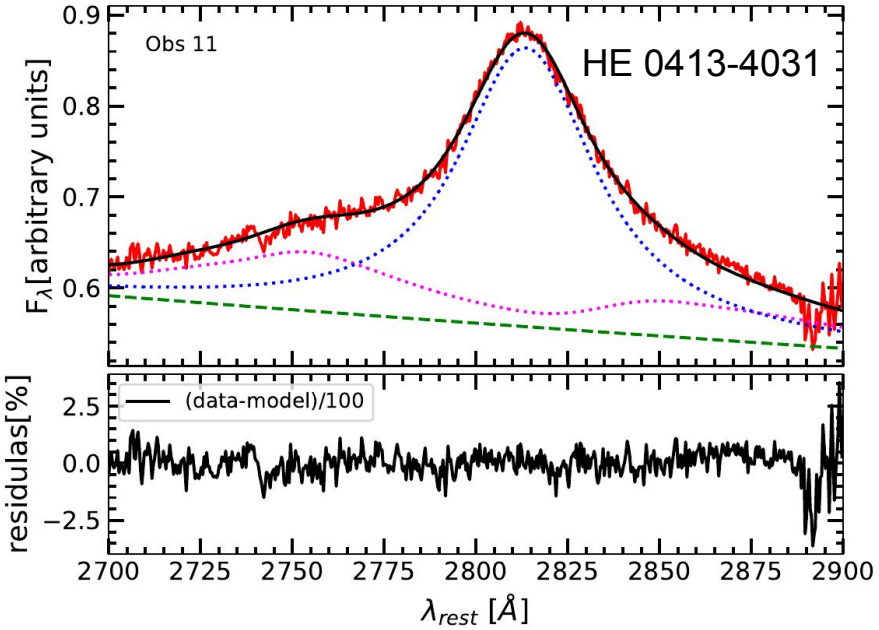

Spectral Modeling

- Our monitoring is focused on Mg II emission line. This is a strong emission line similar to Hβ but located at 2800 Å at rest frame.
- Spectral modeling is done for a narrow band 2700-2900 Å in the rest frame
- Spectrum consists of three basic components: a power-law continuum, broad Mg II emission line, and Fe II pseudo-continuum
- Mg II is described by Gaussian or Lorentzian profile
- For Fe II many templates were tried from Bruhweiler & Verner (2008)

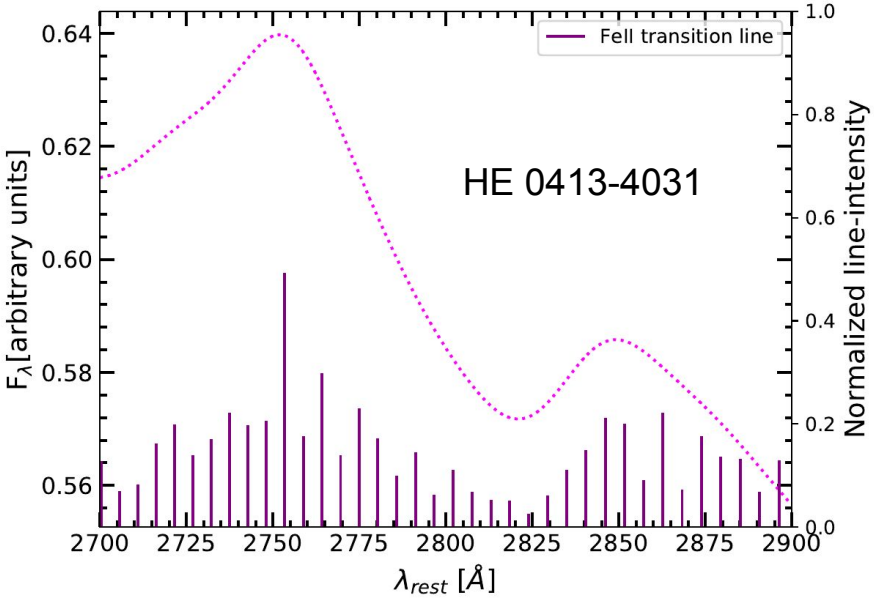

Spectral Modeling

- Single Mg II component does not provide a good fit (checked with all Fe II templates)
- The Mg II line is fitted with a doublet centered at 2796.35 & 2803.53 Å (Modzelewska et al. 2014).
- Best template for Fe II is *d12-m20-20-5*
- This template assumes a cloud number density of 10^{12} cm^{-3} , a turbulent velocity of 20 km s^{-1} , and flux of the hydrogen-ionizing photons of $10^{-20.5}$ cm^{-2} s^{-1} .

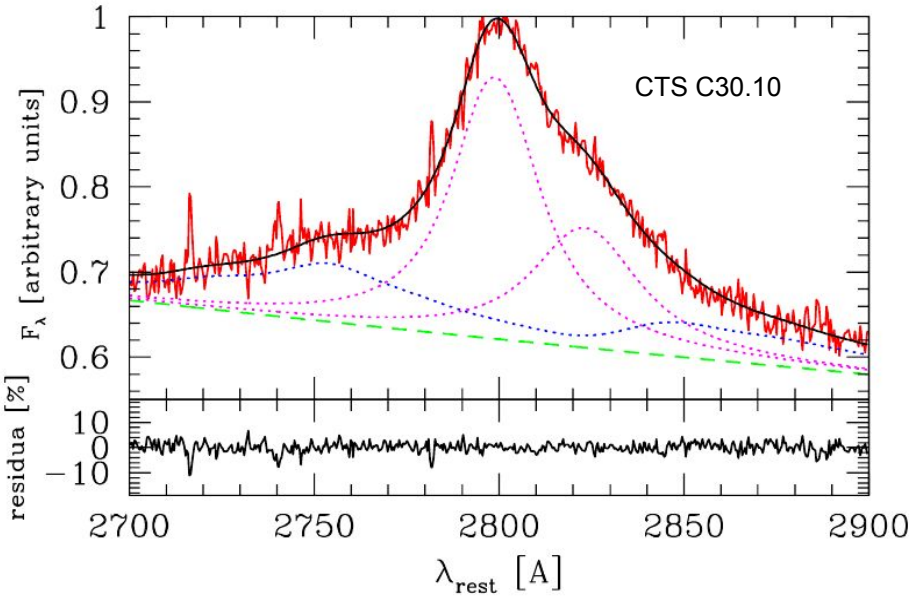

Spectral Modeling

- Best fit template for HE 0413 is *d12-m20-20-5* and for HE 0435 is *d11-m20-21-735*
- Once we have the best template all the observations were fitted for all the three quasars and total Fe II and Mg II fluxes were derived

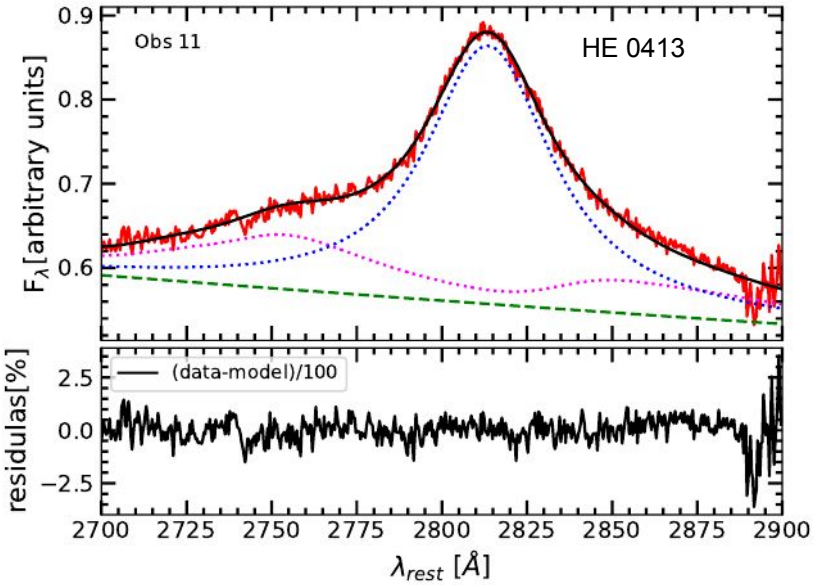

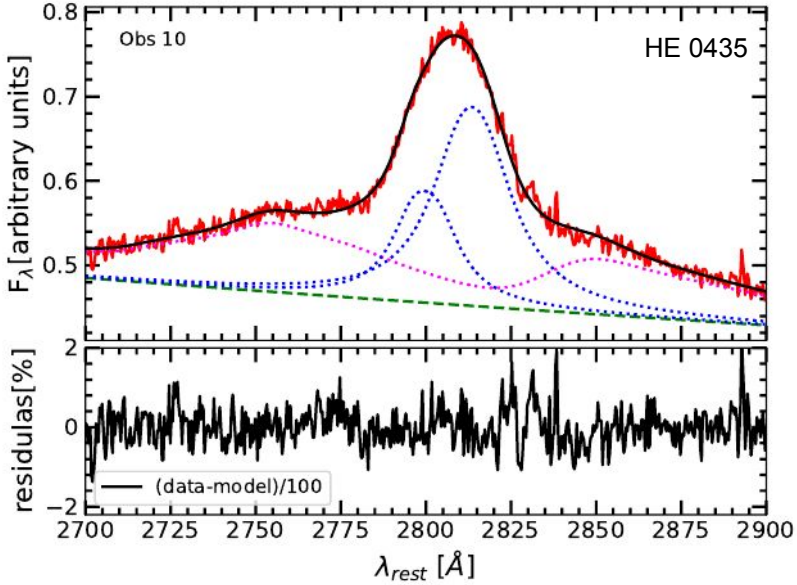

Total Mg II and Fe II light curves

- We have more than 30 observations for each quasars
- Quasi-simultaneous photometric observations are taken from SALTICAM, OGLE, Catalina, Bohum Monitoring Telescope (BMT), and ASAS-SN

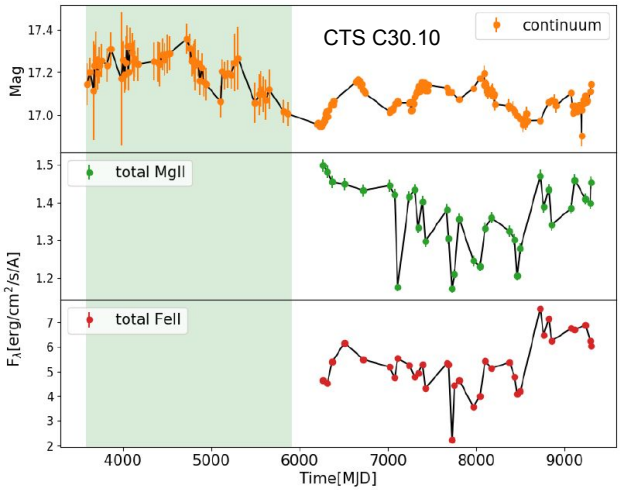

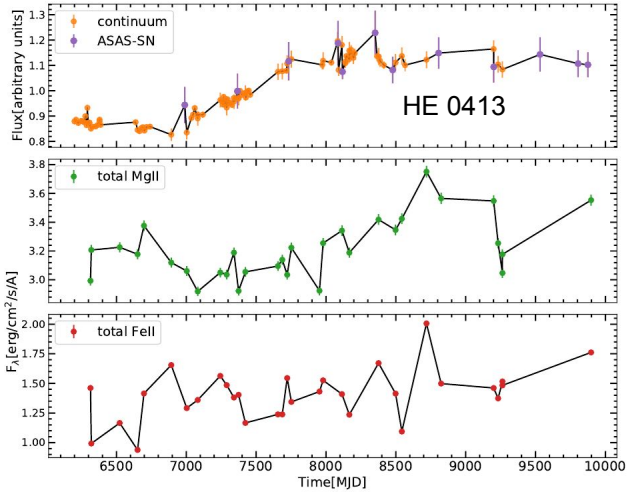

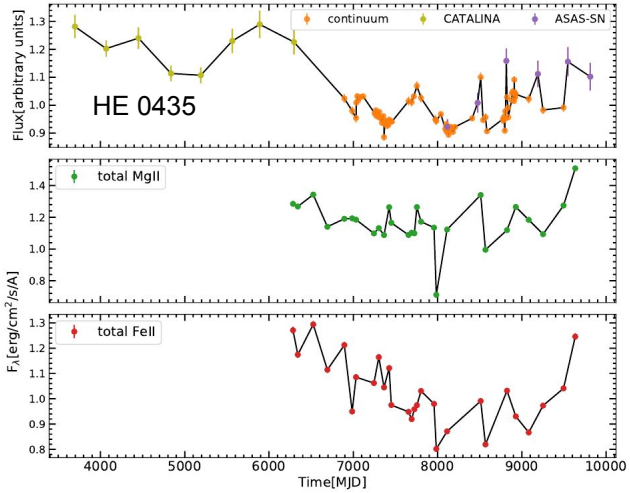

Reverberation Mapping

$$\log R_{BLR} = \text{alpha} + \text{beta} \log L_{44,5100} \quad \text{[days]}$$

Radius-Luminosity relation, beta ~ 0.5

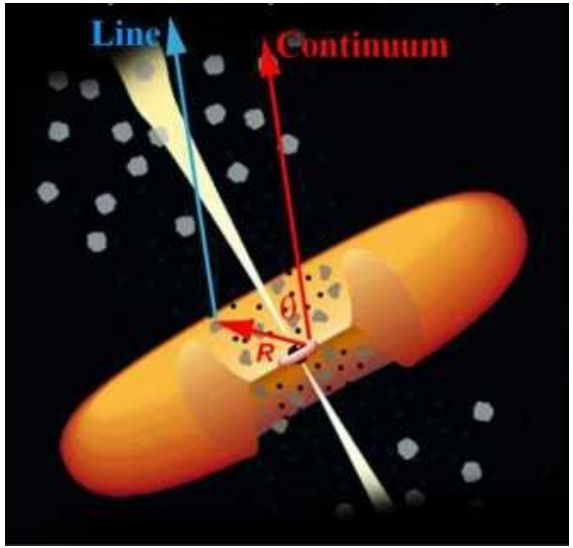

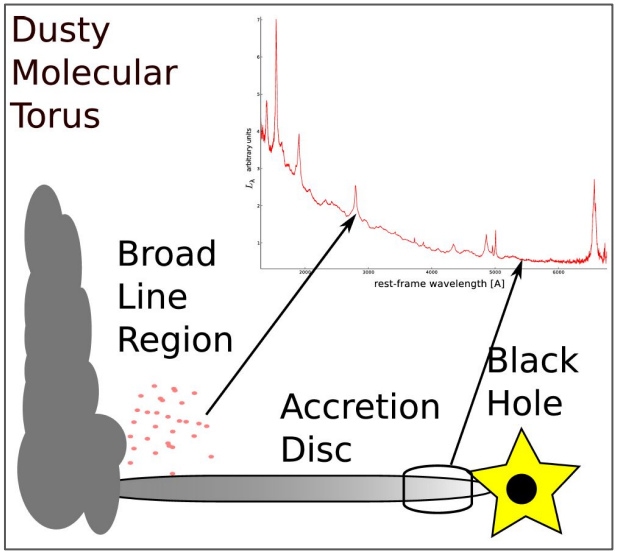

- Size of the Broad Line Region as a function of monochromatic luminosity is predicted by theoretical model
- The size is measured as a delay of the Broad Emission Lines with respect to the variable continuum

Reverberation Mapping

- ICCF, Javelin, Chi-square, zDCF, von-Neumann & Bartels

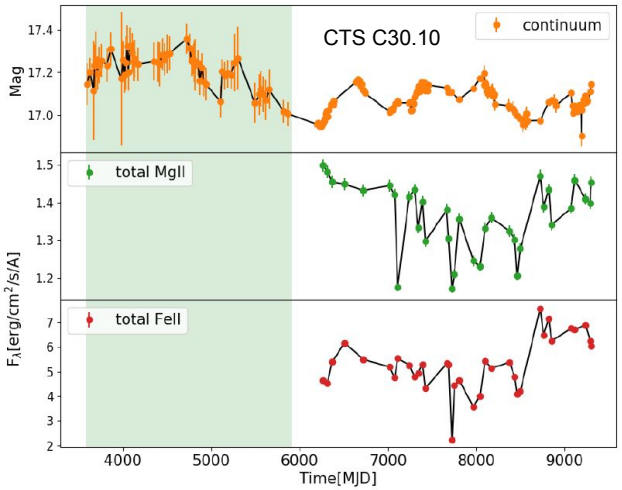

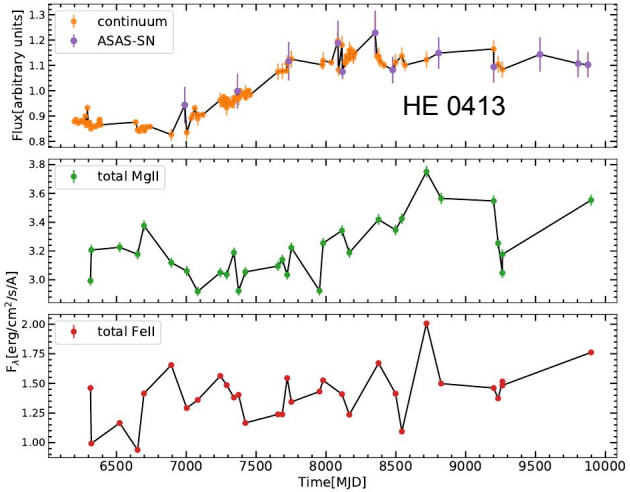

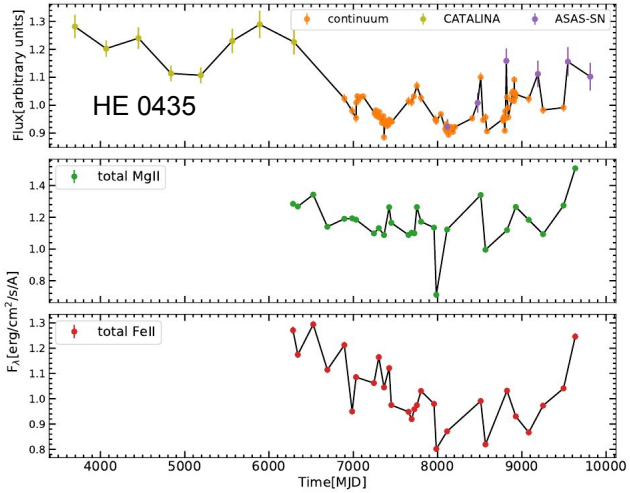

Reverberation Mapping: Results

- We observed time delays for Mg II and Fe II emission lines with respect to continuum for all the three quasars

	Mg II	Fe II
	Rest frame	Rest frame
CTS C30.10:	275^{+12}_{-20} days	270^{+14}_{-25} or 180^{+27}_{-30} days
HE 0413-4031:	314^{+50}_{-56} days	331^{+54}_{-87} days
HE 0435-4312:	281^{+60}_{-74} days	284^{+73}_{-77} days

- The UV Fe II time delays are measured first time for high redshift quasars

Reverberation Mapping: Results

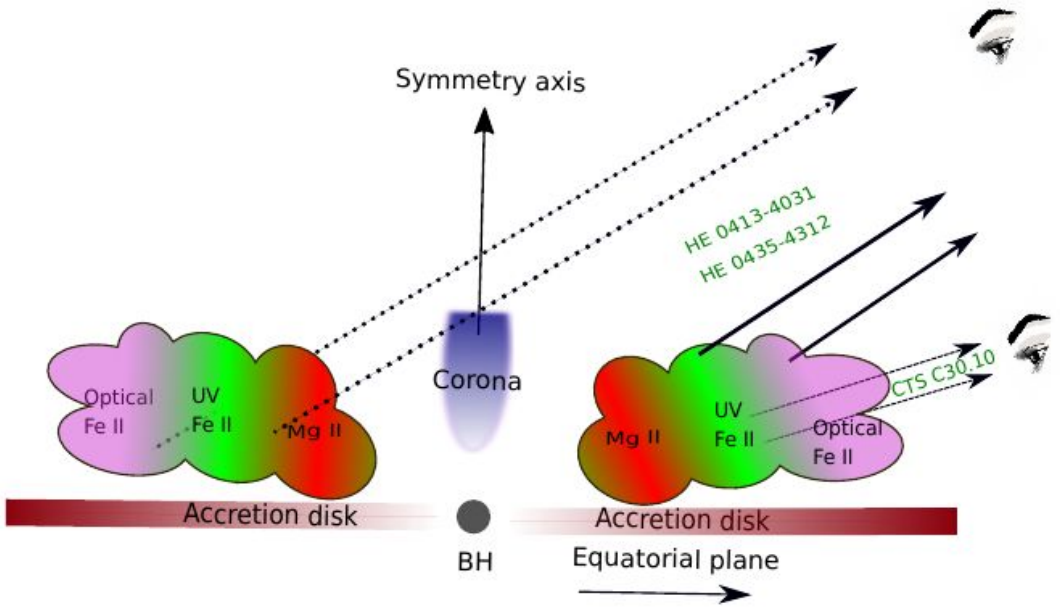

- The shorter time delay for Fe II compared to Mg II in CTS implies that more likely we are seeing the closer part of the BLR and farther part is somehow shielded which is possible when the viewing angle is higher (measured from symmetry axis)
- In HE sources the apparent time delays are higher for Mg II than Fe II suggesting we are also seeing the farther part of the BLR clouds and hence these sources have lower viewing angle

Mg II R-L relation

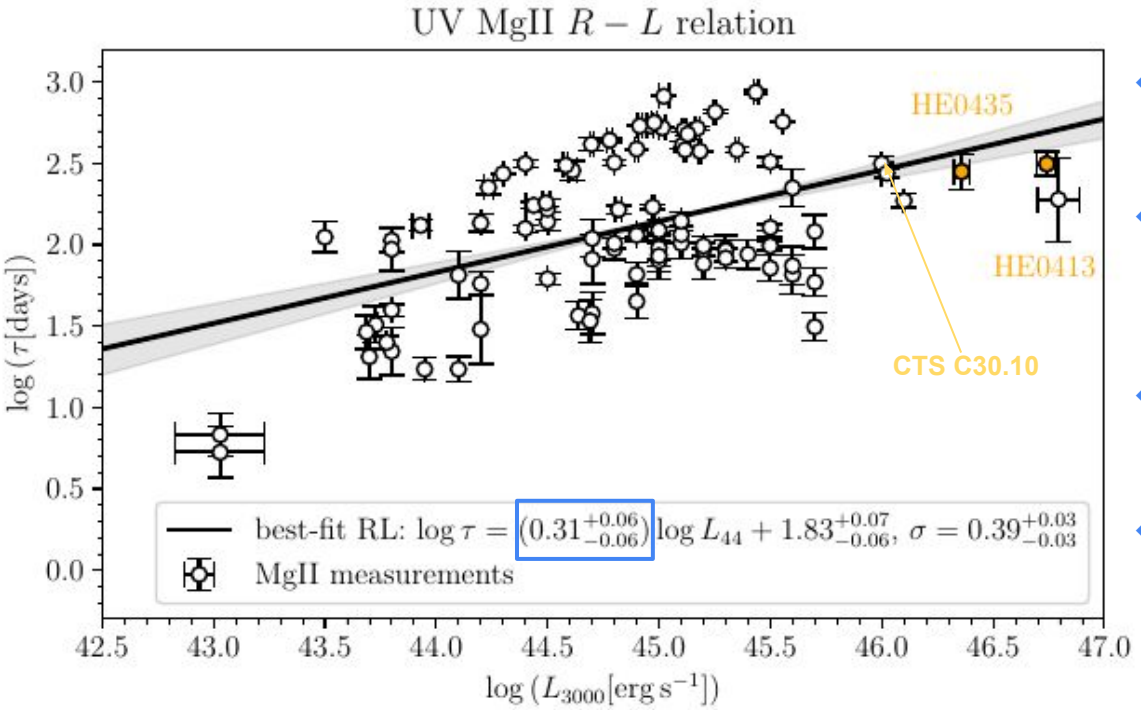

- MgII measurement for high redshift quasars are relatively convenient to measure
- We combined other measurements of Mg II time delays and obtain the updated R-L relation with total 94 quasars (Prince et al. 2023)
- Our three quasars are at the brightest end of the R-L relation which guided the fit
- Massive surveys like SDSS-RM rarely cover the brightest objects

Optical Fe II R-L relation

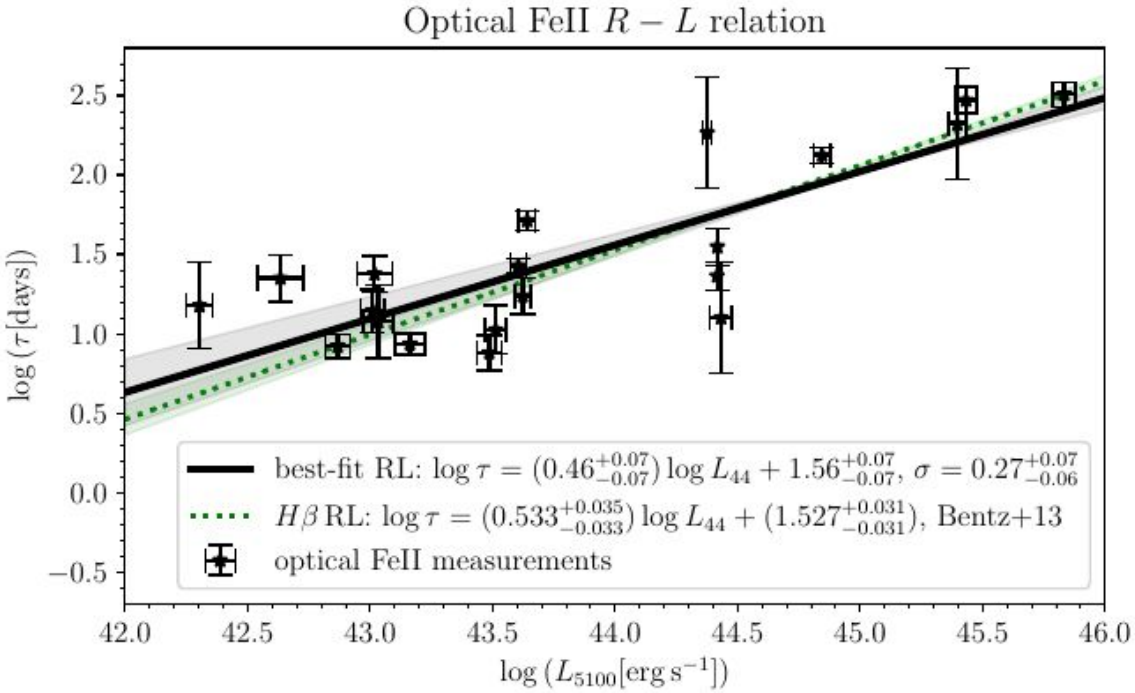

- Optical Fe II time delays were taken from literature but fit was done by us in Prince et al. (2023)
- Green dashed line is the Hβ RL (Bentz et al. 2013)
- Fe II does not seem to be more distant from the back hole than Hβ emission region

Our UV Fe II R-L relation

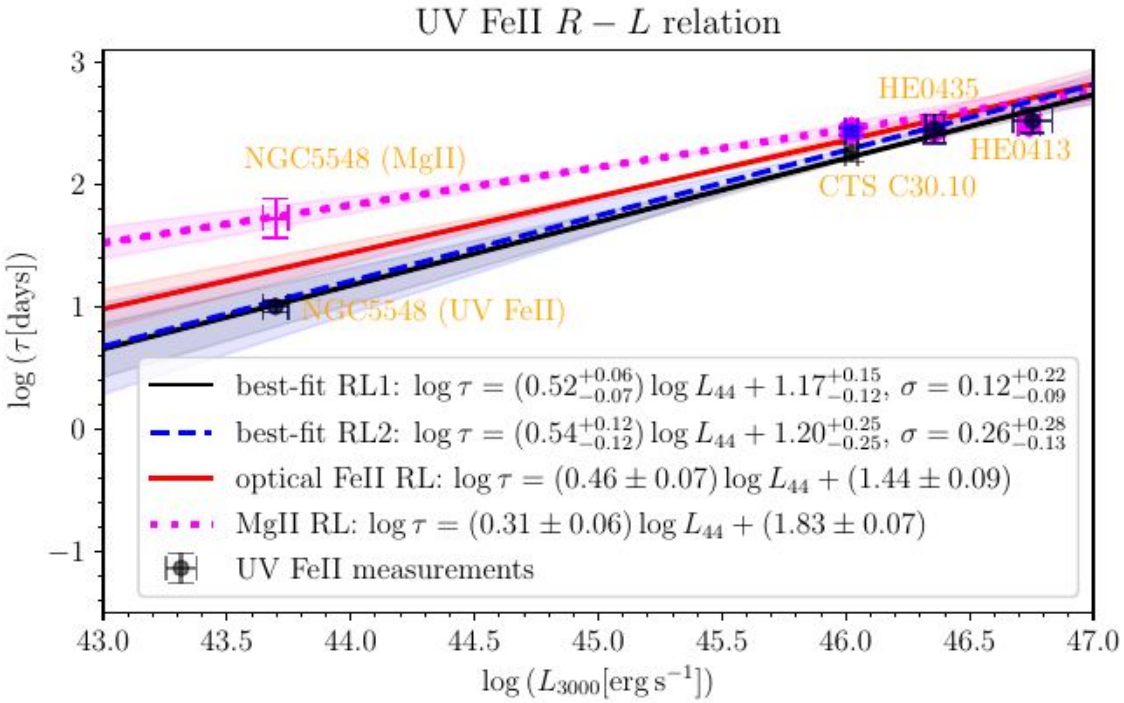

- We have derived the first time the R-L relation for UV Fe II
- The relation is based on our SALT monitoring, plus one old observation of NGC 5548 done with IUE (Maoz et al. 1993)
- The optical Fe II is converted from 5100Å to 3000Å UV monochromatic luminosity for a better comparison
- We clearly see the vertical offset, with UV Fe II being located closer to the SMBH by a factor of ~ 1.8
- Kovacevic-Dojcinovic & Popovic (2015) estimated the mean FWHM for optical and UV Fe II as 2360 $\mathrm{kms^{-1}}$ & 2530 $\mathrm{kms^{-1}}$ which translates to their separation of 1.15

Our UV Fe II R-L relation

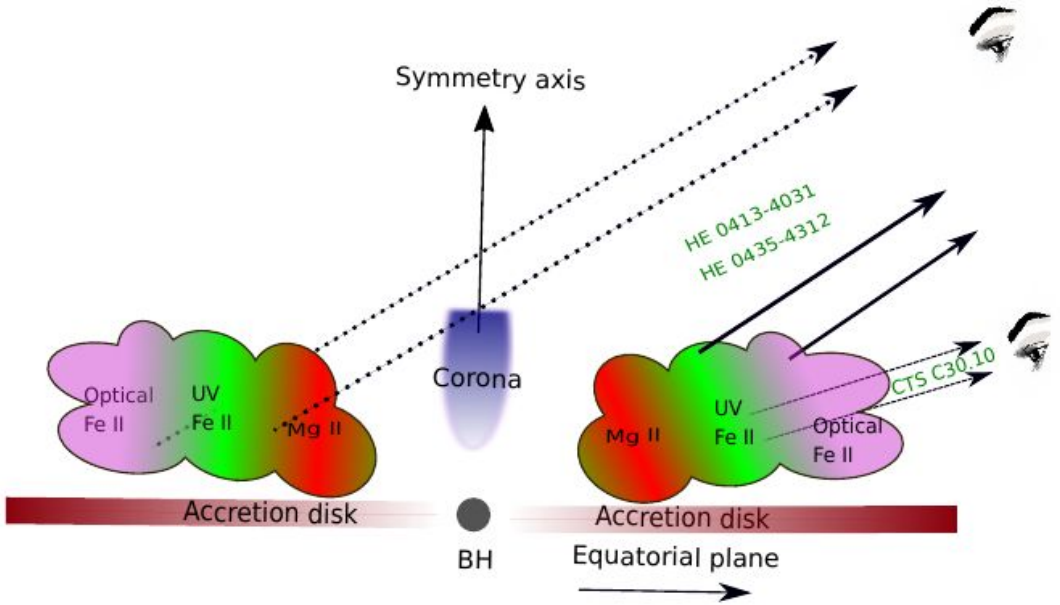

- A vertical offset between the two R-L relations is apparent, which corresponds to the potential mean size difference between the optical FeII-emitting region and the UV FeII-emitting region of $R_{FeII-opt} \sim (1.7 - 1.9)R_{FeII-UV}$, assuming the same slope of $\gamma = 0.5$ within the uncertainties

Mg II emission line drift

- A small fraction of quasars showed systematic drift in their emission lines (Liu et al. 2014).
- The trend, if interpreted formally as a linear shift, implies a change of the line position by 0.97 ± 0.13 Å/yr, or an acceleration of 104 ± 14 km s^{-1} yr^{-1} in the quasar rest frame, assuming a redshift z = 1.2231.
- This is vigorously discussed as an evidence of compact binary supermassive black hole system in the nucleus.

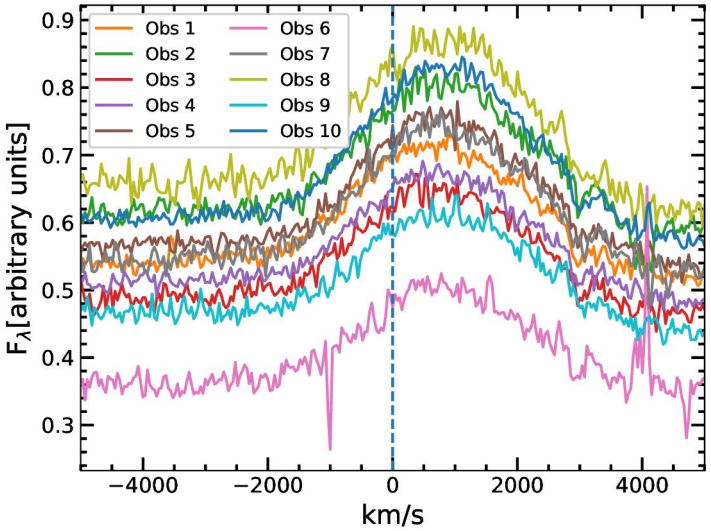

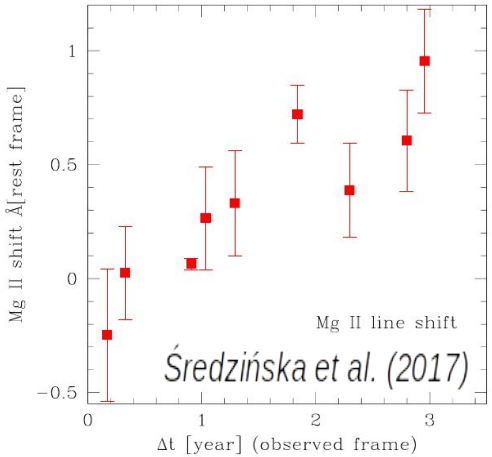

Fig. 5. Shift of the Mg II line in Observations 1 to 9 with respect to Observation 10, calculated directly from the data (see Sect. 4.1).

Our UV Fe II R-L relation

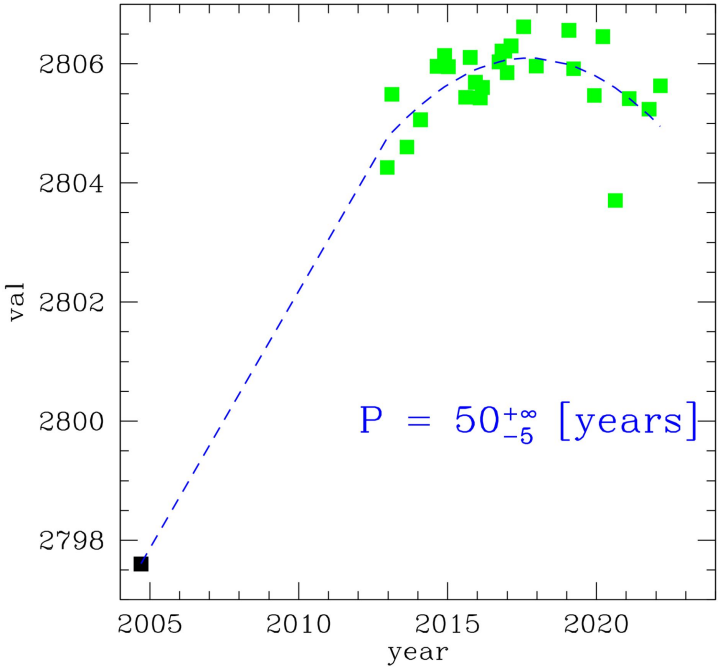

- Fit to the data up to 2022, few more observations are there that needs to be included
- We do not yet see periodicity. We would likely need another 20 years of data...
- But the period (22 years in the rest frame) would locate the second black hole quite close (at some 300 Rg for the black hole mass of log M = 9.3 in this source). And we do not see a considerable distortion in the broad band spectrum of the quasar...

Summary

- Mg II and Fe II emission lines were measured in intermediate redshift quasars
- We measured the time delays of hundreds of days between the Mg II or Fe II and continuum in these exceptionally bright sources
- This allowed us to construct the Radius-Luminosity relation for Mg II which can be used for mass measurements in intermediate redshift quasars
- We also obtain the R-L for the first time for UV Fe II, this helps us to disentangle the Mg II and Fe II emission regions
- We also detect a possible shift in Mg II emission lines in one of the quasars suggesting a potential binary black hole system

References

Modzelewska, J., Czerny, B., Hryniewicz, K., et al. 2014, A&A, 570, A53
Średzińska, J., Czerny, B., Hryniewicz, K., et al. 2017, A&A, 601, A32
Czerny, B., Olejak, A., Rałowski, M., et al. 2019, ApJ, 880, 46
Prince, R., Zajacek, M., Czerny, B., et al. 2022, A&A, 667, A42
Prince, R., Zajacek, M., Panda, S., Czerny, B., et al. 2023, A&A (in press)

References

Modzelewska, J., Czerny, B., Hryniewicz, K., et al. 2014, A&A, 570, A53
Średzińska, J., Czerny, B., Hryniewicz, K., et al. 2017, A&A, 601, A32
Czerny, B., Olejak, A., Rałowski, M., et al. 2019, ApJ, 880, 46
Prince, R., Zajacek, M., Czerny, B., et al. 2022, A&A, 667, A42
Prince, R., Zajacek, M., Panda, S., Czerny, B., et al. 2023, A&A (in press)

Thank you for your attention!

Back-up: Our UV Fe II R-L relation

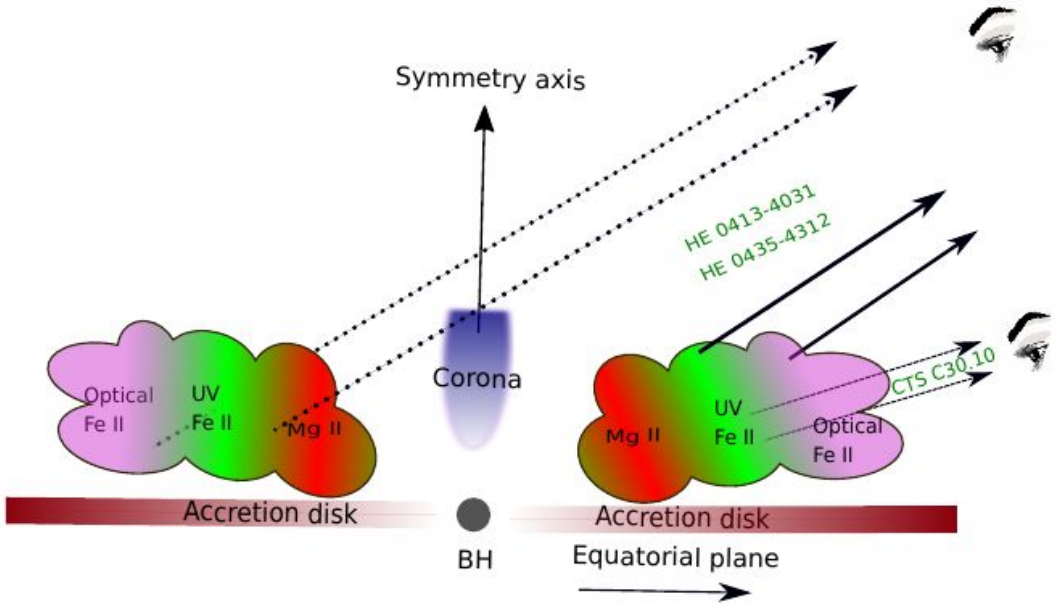

- A vertical offset between the two R-L relations is apparent, which corresponds to the potential mean size difference between the optical FeII-emitting region and the UV FeII-emitting region of $R_{FeII-opt} \sim (1.7 - 1.9)R_{FeII-UV}$, assuming the same slope of $\gamma = 0.5$ within the uncertainties

Back up: Spectral Modeling

Pseudo-continuum UV FeII emission profile (dotted magenta) obtained by smearing the FeII transition lines (purple) by a velocity profile of 2820 km/s for HE 0413-4031 (left panel) and 2350 km/s for HE 0435-4312 (right panel). Transition lines are theoretical predictions taken from FeII templates (Bruhweiler & Verner 2008) `d12-m20-20-5.dat` for HE 0413-4031 and `d11-m20-20.5-735.dat` for HE 0435-4312

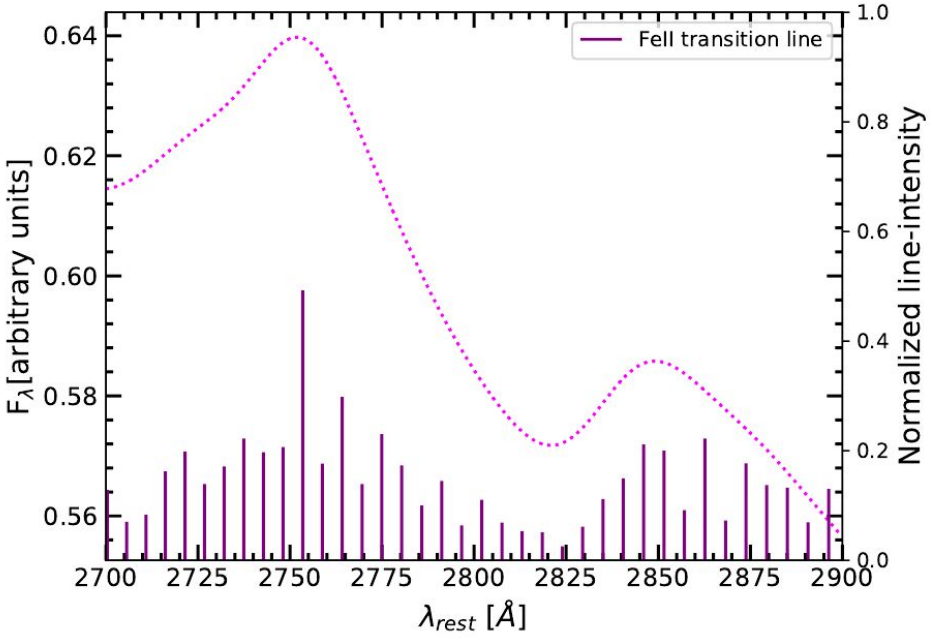

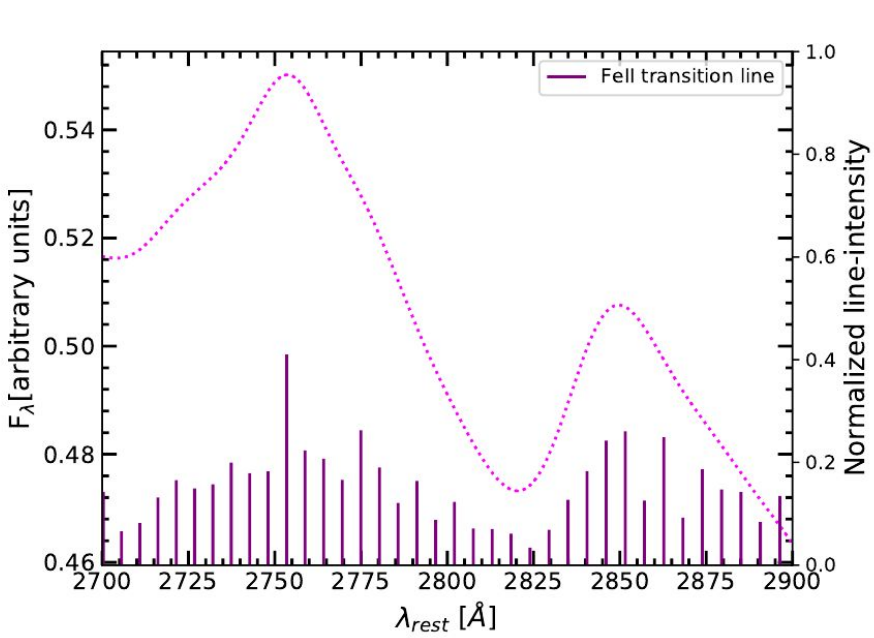

Back up: UV Fe II modeling

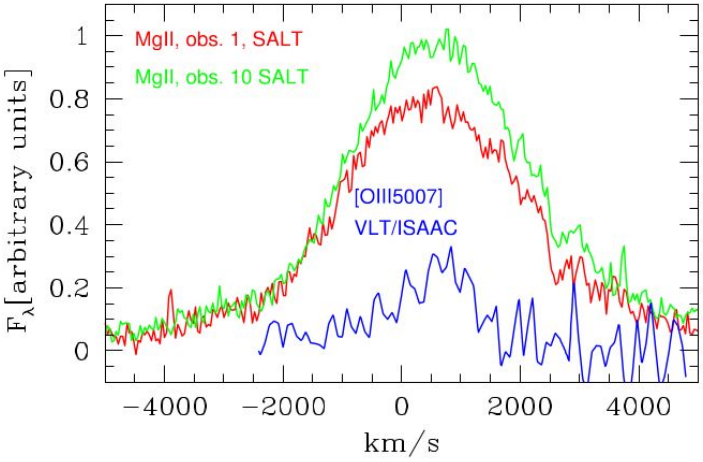

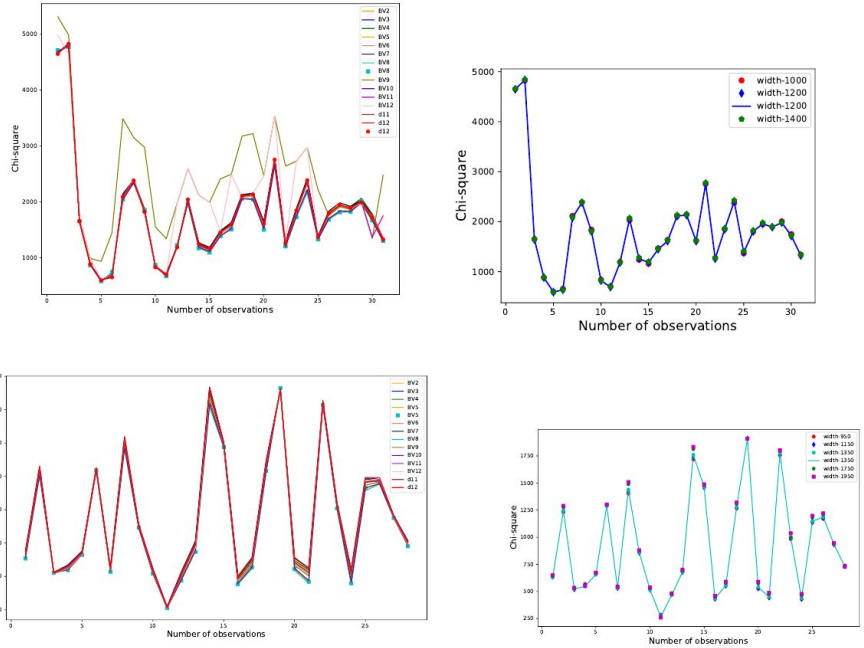

g. D.1. The left panel represents the chi-square distribution of different templates that have been used to model the UV Fe II emission. ne right panel shows the chi-square distribution when various equivalent widths were chosen to model the UV FeII. The upper panel d lower panel are for HE 0413 and HE 0435 sources.